Supporting information for

Reversible ligation of programmed DNA-gold nanoparticle assemblies

Pascal K. Harimech,[†] Simon R. Gerrard,[‡] Afaf H. El-Sagheer[§,◊], Tom Brown*[,§] and Antonios G. Kanaras*[,†]

[†] Physics and Astronomy, Faculty of Physical Sciences and Engineering, University of Southampton, Southampton, SO17 1BJ, United Kingdom

[‡] Chemistry, Faculty of Natural and Environmental Sciences, University of Southampton, Southampton, SO17 1BJ, United Kingdom

[§] Department of Chemistry, University of Oxford, Chemistry Research Laboratory, Oxford, OX1 3TA, United Kingdom

[◊] Chemistry Branch, Department of Science and Mathematics, Faculty of Petroleum and Mining Engineering, Suez University, Suez 43721, Egypt

Table of contents:

S1. Materials and Methods

Commercially available reagents and solvents were purchased from Sigma-Aldrich and used without further purification unless stated otherwise: Sodium tetrachloroaurate (III) dehydrate, trisodium citrate, sodium chloride, boric acid, sodium phosphate monobasic, sodium phosphate dibasic, tris(hydroxymethyl) aminomethane (TRIS), ethylene diamine tetraacetic acid disodium salt dehydrate (EDTA), formamide, agarose (low EEO), Ficoll® 400, and *bis*(p-sulfonatophenyl)phenyl phosphine dehydrate dipotassium salt (BSPP). 3-(2-Cyanoethenyl)-9-(2'-deoxyribofuranosyl) carbazole was purchased from Berry & Associates, Inc. (MI, USA).

Oligonucleotides were synthesized by ATDBio Ltd. using standard solid phase phosphoramidite methods and were purified by RP-HPLC. All reactions were carried out using Milli-Q water with a resistivity ≥18.2 MΩ·cm unless stated otherwise. All glassware and stirrer bars were rinsed with Aqua regia followed by Milli-Q water.

UV – visible spectra were recorded on a Shimadzu 100 UV-Vis spectrophotometer with a step size of 1 nm. The photo-crosslinking reaction was performed with a UVP CX-2000 equipped with 5 UV lamps with 8 W each. TEM images were obtained on a FEI Tecnai T12 transmission electron microscope operating at a bias voltage of 80 kV. Sample preparation involved deposition and evaporation of a 10µL droplet onto a grid (Formvar- and carbon-coated 400 mesh copper grid). Hydrodynamic radii were recorded with a Malvern Zetasizer Nano ZS.

Gold nanoparticle preparation

Spherical gold nanoparticles of 15 nm were synthesized according to the well-established Turkevich method.[1] In detail, a $NaAuCl_4$ solution (100 mL, 1 mM) was brought to the boil. Subsequently, a boiling trisodium citrate solution (5 mL, 77.5 mM) was added rapidly under vigorous stirring. A color change from colorless through purple to wine red indicated the formation of gold nanoparticles. The solution was boiled for another 15 min and then left to cool to room temperature. BSPP (15 mg, MW: 534.62 g/mol) was added under stirring and the solution was left to stir for at least 16 hours. The ligand increases stability against high ionic strength media by preventing the gold nanoparticles from irreversibly aggregating. The BSPP-coated gold nanoparticles were filtered through a 0.2 µm syringe filter to remove larger aggregates. Sodium chloride was added until the solution became brown-blue and it was centrifuged for 5 min at 5000 rpm. The supernatant was removed completely and the pellets were re-dispersed in a total volume of 3 mL de-ionized water yielding nanoparticle concentrations of 300 nM. The concentration was determined using Beer-Lambert's law, using published size-dependent extinction coefficients for gold nanoparticles.[2]

DNA attachment to gold nanoparticles

Gold nanoparticles were mixed with the oligonucleotides in buffered solution (20 mM sodium phosphate buffer, 50 mM NaCl, pH 7.4). Typically, 30 pmol of gold nanoparticles in a total volume of 200 µL were used. It was found that ratios close to 1:1 nanoparticle: DNA gave the highest yield of mono-conjugated gold nanoparticles. BSPP solution (10 µL, 50mg/mL) was added in order to cleave the disulfide bond of the linker (See **Figure S4**). After an incubation time of 1 hour, the gold nanoparticles were separated according to the number of attached strands by agarose gel electrophoresis (2.25%, 90 V, 60 min) in

0.5x Tris/Borate/ EDTA (TBE). TBE is prepared by mixing 54g of tris base, 27.5 g of boric acid and 20ml of 0.5M EDTA at pH 8.0. The desired bands were cut from the gel and soaked in 0.5xTBE buffer overnight, while gently shaking in order to allow the nanoparticles to diffuse out of the gel into solution. The solution was then filtered through a 0.2 µm syringe filter to remove small gel pieces and afterwards centrifuged at 16400 rpm for 10 min (25000 G) to concentrate the mono-conjugates. The concentration was again measured by UV-Visible spectroscopy as described before.

DNA-Nanoparticle assemblies

DNA-Nanoparticle dimers: Gold nanoparticle dimers were made by mixing two different types of mono-conjugates in buffer (20 mM sodium phosphate buffer, 60 mM NaCl, pH 7.4). The solution was heated to 65 °C for 5 min and shaken occasionally (every 2-3 min). Subsequently, the solution was left to cool to room temperature and three cycles of heating and cooling were repeated to maximize the yield of DNA hybridization. The nanoparticle assemblies were purified by gel electrophoresis in a 1.75% agarose gel (90 V, 30 min) in 0.5x TBE.

DNA-Nanoparticle trimers: Gold nanoparticle trimers were made by mixing three different nanoparticle batches of mono-conjugates in buffer (20 mM sodium phosphate buffer, 60 mM NaCl, pH 7.4), and subsequent experimental steps were taken as for the formation of nanoparticle dimers.

DNA-Nanoparticle tetrahedral structures: Gold nanoparticle tetrahedral structures were made by mixing the two different sets of photo-crosslinked nanoparticle dimers in equimolar ratios in buffer (20 mM sodium phosphate buffer, 60 mM NaCl, pH 7.4) and subsequent experimental steps were taken as for the formation of nanoparticle dimers and trimers.

DNA crosslinking

DNA crosslinking was carried out in a photo-crosslinker by irradiation with UV-A light (centered at 365 nm, 50 mW/cm^2, 15 min) with the samples being in a 1.5 mL polypropylene tube in an ice-bath at a distance of 4 cm from the UV lamp. The reverse reaction was carried out with UV-B light (centered at 312 nm, 50 mW/cm^2, 15 min) under the same conditions.

Denaturing conditions and gel electrophoresis

In order to de-hybridize non-crosslinked gold nanoparticle assemblies, formamide was added up to a maximum of 30% v/v. In addition, the assemblies were heated for 5 min at 70°C and rapidly cooled in an ice-bath. The reference samples were mixed with a Ficoll® 400 solution (final concentration of 3% v/v). The gold nanoparticle assemblies were then run in a 1.75% agarose gel for 30 min.

S2. DNA sequences and chemical modifications

The DNA sequences employed in this work are listed in **Table S1**. Each oligonucleotide consists of three parts which are complementary by 26 bp to each of the other strands and bridged by three thymine bases to reduce strain at the corners of the tetrahedron. The structures of the DNA thiol-modification and the cyanovinyl carbazole nucleoside are shown in **Figures S1** and **S2**. The DNA sequences were modified to incorporate crosslinking sites on each of the edges of the tetrahedra. The three-dimensional display of the tetrahedron formed by all four DNA strands is depicted in **Figure S3**.

1	5'-HSC_6H_{12}-TTT GCC TGG AGA TAC A**X**A CAC ATT ACG GC TTT CCC TAT TAG AAG A**X**A TCA GGT GCG CG TTT CGG TAA GTA GAC GG**T** *G***T**C AGT TCG CC
2	5'-HSC_6H_{12}-TTT CGC GCA CCT GAT *G*TC TTC TAA TAG GG TTT GCG ACA GTC GTT CA**X** ATA GAA TGC CC TTT GGG CTG TTC CGG GT*G* TGG CTC GTC GG
3	5'-HSC_6H_{12}-TTT GGC CGA GGA CTC T*G*T CTC CGC TGC GG TTT GGC GAA CTG A**X**A CCG TCT ACT TAC CG TTT CCG ACG AGC CA**X** ACC CGG AAC AGC CC
4	5'-HSC_6H_{12}-TTT GCC GTA ATG TG**T** *C***T**G TAT CTC CAG GC TTT CCG CAG CGG AGA **X**AG AGT CCT CGG CC TTT GGG CATT CTA **T***G***T** GAA CGA CTG TCG

Table S1: The oligonucleotide sequences used in this work. The positions of the cyanovinyl carbazole modification are marked as a **bold X**. The base directly opposite X is marked in italics.

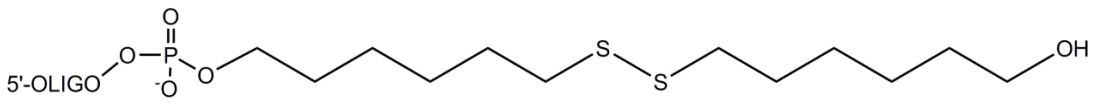

Figure S1: 5'-Disulfide modification.

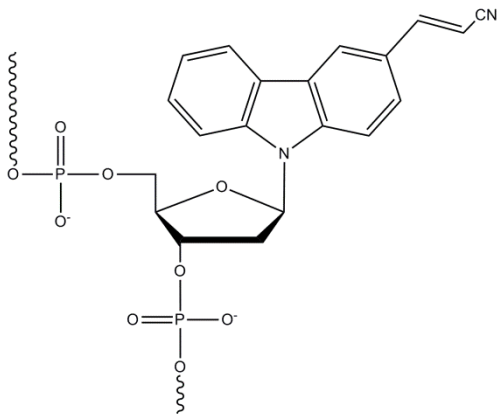

Figure S2: 3-Cyanovinyl carbazole nucleoside modification.

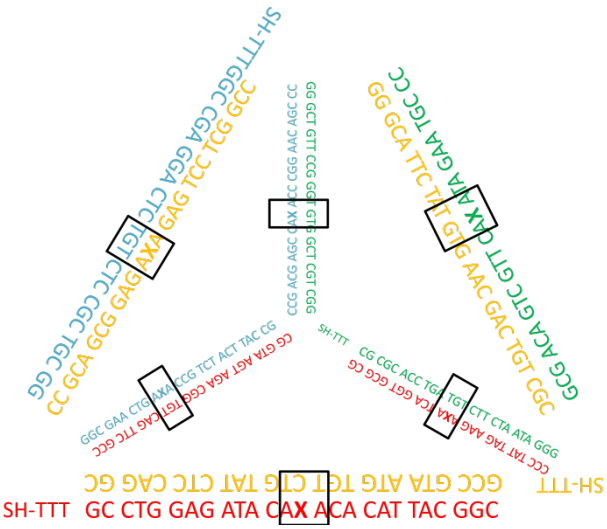

Figure S3: Three-dimensional view of the tetrahedral structure formed when all four oligonucleotide strands are combined. The boxes indicate where the DNA is modified with cyanovinyl carbazole so that crosslinking can occur.

S3. Reaction mechanisms

The reaction mechanism of the disulfide cleavage of protected thiol modified DNA with BSPP is shown in **Figure S4**. The crosslinking reaction and its mechanism are shown in **Figure S5**. UV-light excites the C-C double bond in the thymine base (1) to a triplet (2) which then forms an exciplex with the vinyl group of the cyanovinyl carbazole molecule (3). This exciplex then collapses to a biradical (4) which finally forms the cyclobutane (5). In the last step a re-orientation of the cyano group leads to different stereochemisties. [3,4]

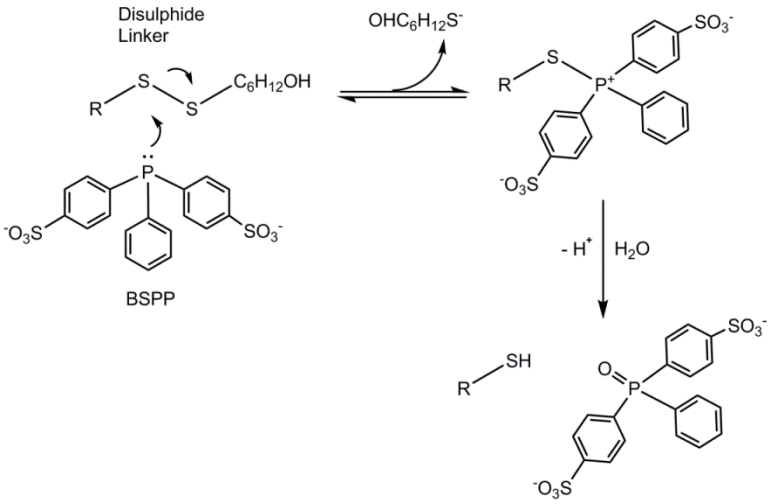

Figure S4: The mechanism of the disulfide cleavage with BSPP.[5]

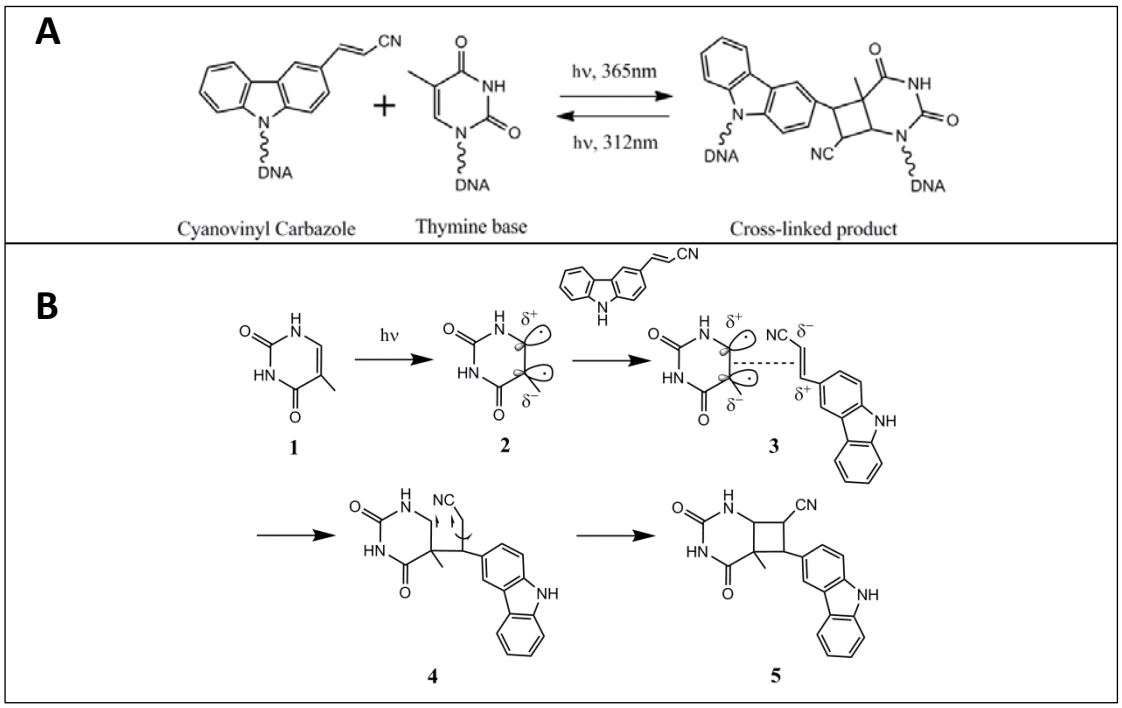

Figure S5: (A) The reversible crosslinking reaction between cyanovinyl carbazole and a thymine base. (B) The reaction mechanism of the [2+2]-photocycloaddition. The stereochemistry is not indicated.

S4. Gold nanoparticle characterization

The size distribution of the BSPP-coated gold nanoparticles was determined by analyzing TEM images with the software ImageJ[#] (**Figure S6**).

UV-Visible spectra were recorded of the gold nanoparticles before and after UV irradiation (**Figure S7**). There was no shift or broadening of the plasmon resonance, which indicates that the particles did not change size or shape upon UV irradiation.

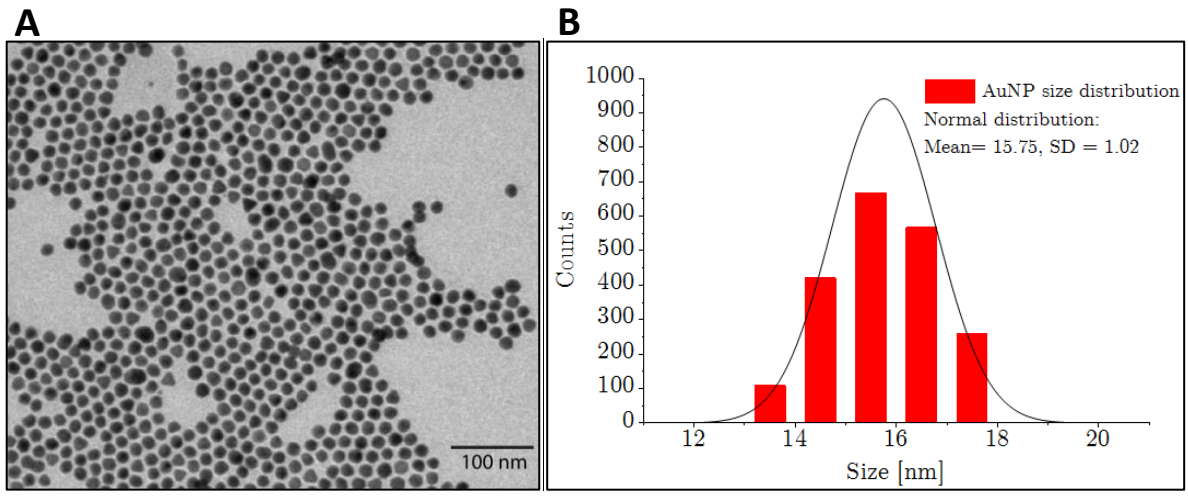

Figure S6: **(A)** TEM image and **(B)** size distribution of the BSPP-coated 15nm gold nanoparticles.

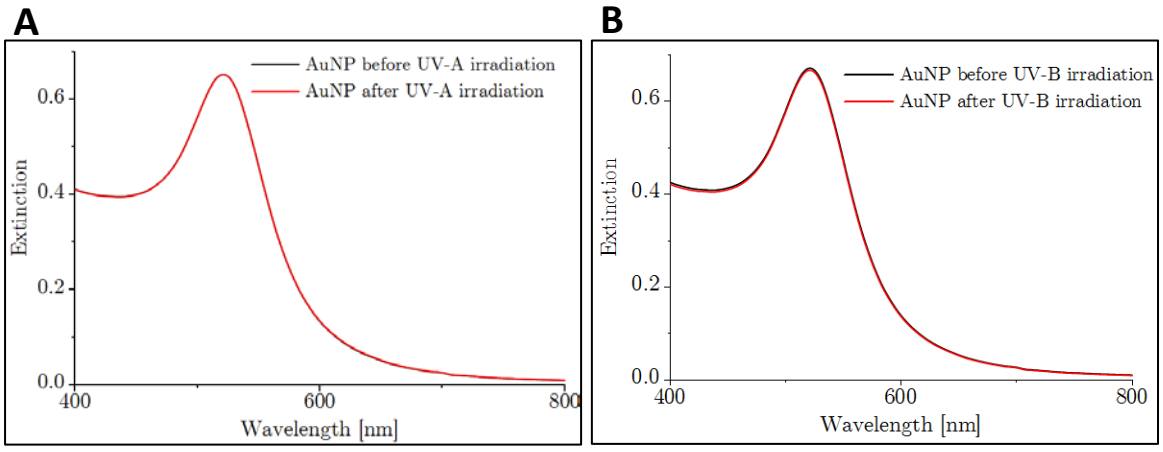

Figure S7: UV-Vis spectra of 15 nm gold nanoparticles before and after irradiation with **(A)** UV-A and **(B)** UV-B light.

[#] Available from: http://imagej.nih.gov/ij/

S5. Gold nanoparticle assemblies: dimers

The structures of the two types of dimers assembled for the formation of the tetrahedra are depicted in **Figure S8**. The dimers were assembled using the oligonucleotides 1+2 and 3+4 (*cf.* **Table S1**), which yield dimers with equivalent properties. An additional zoomed out TEM image is provided in **Figure S9**.

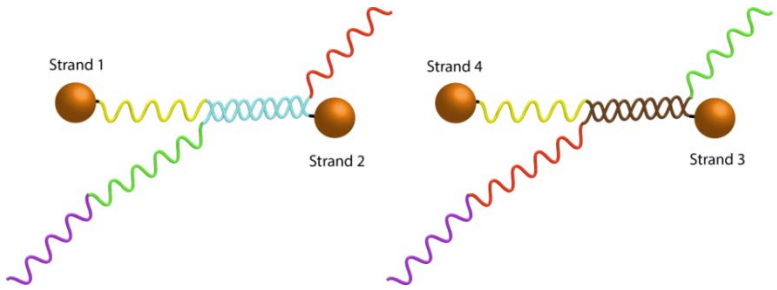

Figure S8: The two structures of the two types of dimers used for tetrahedral formation. The colors highlight the three different parts of the oligonucleotides as described in Section S2.

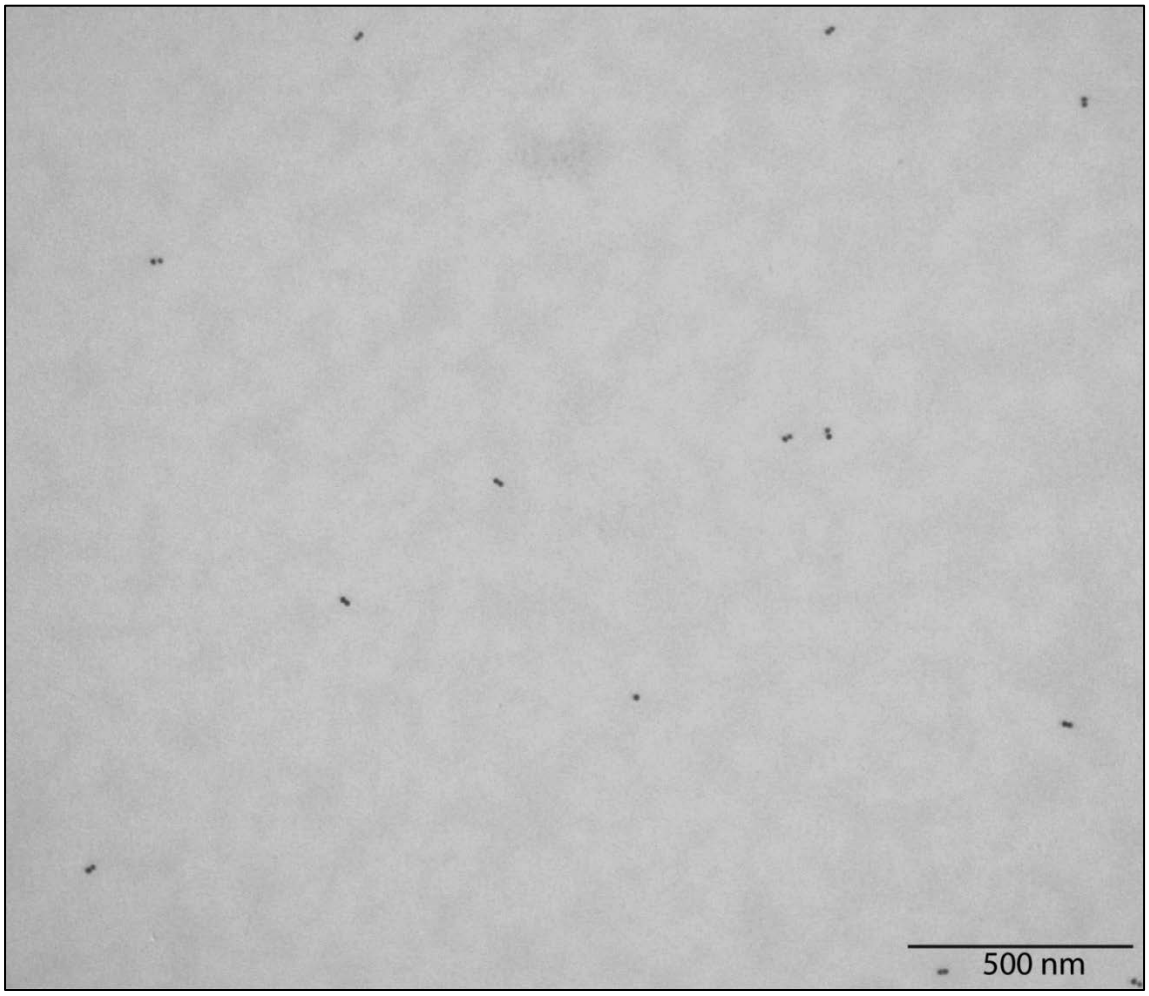

Figure S9: Additional TEM image of crosslinked gold nanoparticles dimers over a larger area of the grid.

S6. Gold nanoparticle assemblies: trimers

Figure S10 shows the structure of the gold nanoparticle trimer with the oligonucleotides 1+2+3 (*cf.* **Table S1**). In **Figure S11**, an agarose gel displays the crosslinking reactions on the gold nanoparticle trimers. Lanes 1 and 2 are loaded with mono-conjugates and dimers respectively and act as control experiments. Similar to the dimer gel, electrophoretic mobility of both the crosslinked and re-crosslinked trimers (Lanes 3, 5) is retarded with respect to the de-crosslinked trimers (Lane 4), which run as fast as the mono-conjugate band.

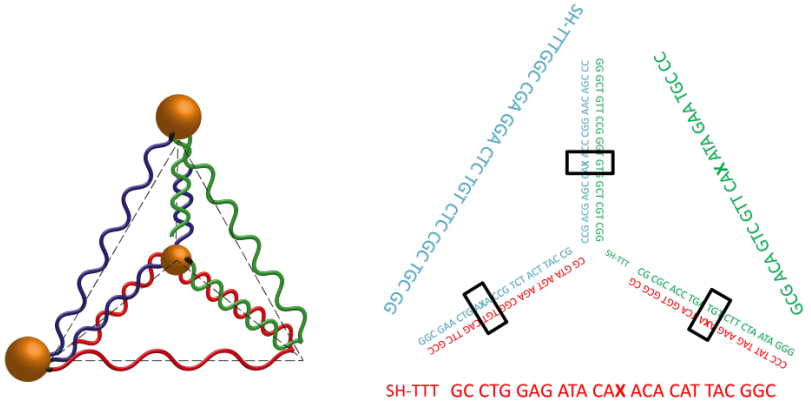

Figure S10: One configuration of gold nanoparticle trimers when three different oligonucleotides are applied. Each color represents one oligonucleotide strand. The boxes indicate where crosslinking can occur.

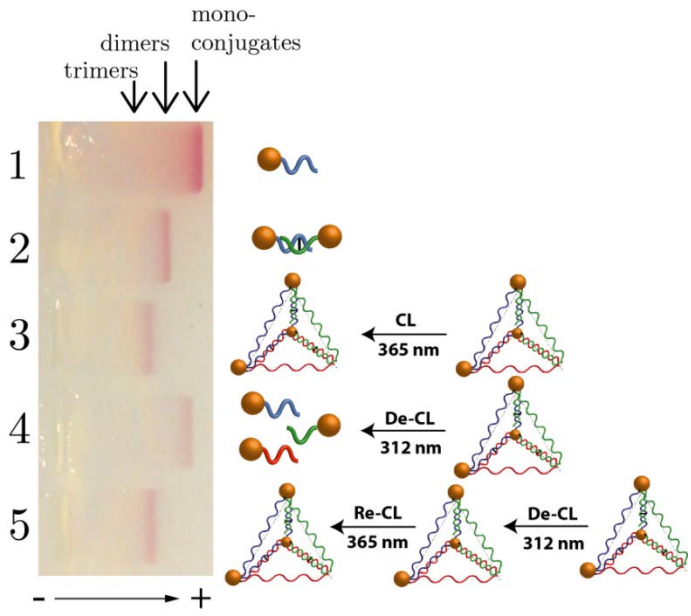

Figure S11: An agarose gel comparing crosslinked and de-crosslinked trimers with mono-conjugates and dimers in denaturing conditions. *Lane 1*: reference mono-conjugates; *Lane 2*: reference dimers; *Lane 3*: crosslinked trimers; *Lane 4*: de-crosslinked trimers; *Lane 5*: re-crosslinked trimers.

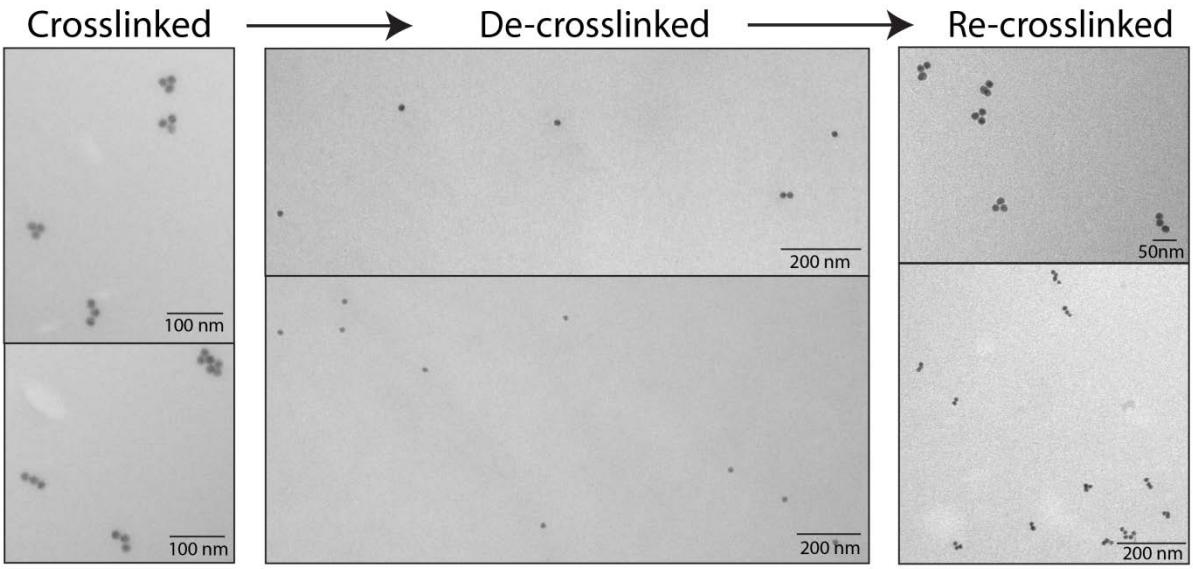

Figure S12: TEM images of crosslinked trimers, de-crosslinked trimers and re-crosslinked trimers.

Figure S13: Additional TEM image of crosslinked gold nanoparticles trimers over a larger area of the grid.

S7. Gold nanoparticle assemblies: tetrahedral structure

The assembly and crosslinking reactions of gold nanoparticle tetrahedral structures are discussed in this section. **Figure S14** shows the structure of the gold nanoparticle tetramer where all four DNA strands are employed. In **Figure S15**, an agarose gel displays the crosslinking reactions on the gold nanoparticle tetramers. Lanes 1-3 are loaded with mono-conjugates, dimers and trimers respectively and act as control experiments. Similar to the dimer and trimer gels, mobility of both the crosslinked and re-crosslinked tetrahedra (Lanes 4, 6) is retarded with respect to the de-crosslinked tetrahedra (Lane 5), which run as fast as the mono-conjugate band.

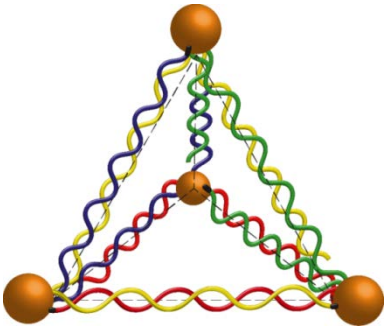

Figure S14: Scheme for the gold nanoparticle tetramers formed when all four oligonucleotides are utilized. Each color represents one oligonucleotide.

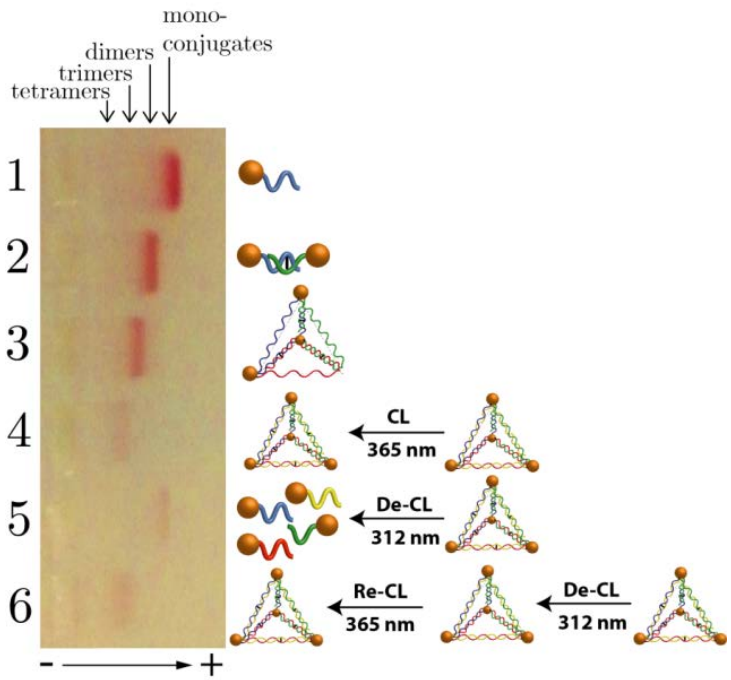

Figure S15: An agarose gel comparing crosslinked and de-crosslinked tetramers with mono-conjugates, dimers and trimers in denaturing conditions. *Lane 1*: reference mono-conjugates; *Lane 2*: reference dimers; *Lane 3*: reference trimers; *Lane 4*: crosslinked tetramers; *Lane 5*: de-crosslinked tetramers; *Lane 6*: re-crosslinked Tetramers.

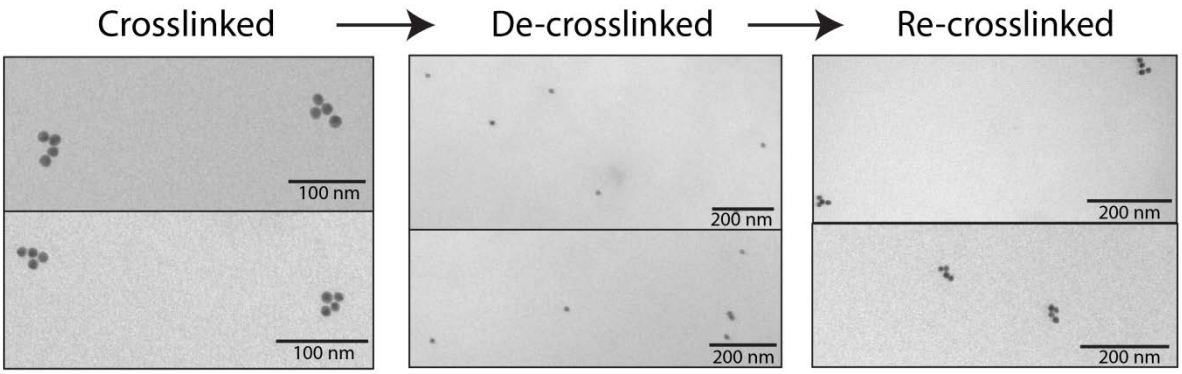

Figure S16: TEM images of crosslinked tetrahedra, de-crosslinked tetrahedra and re-crosslinked tetrahedra.

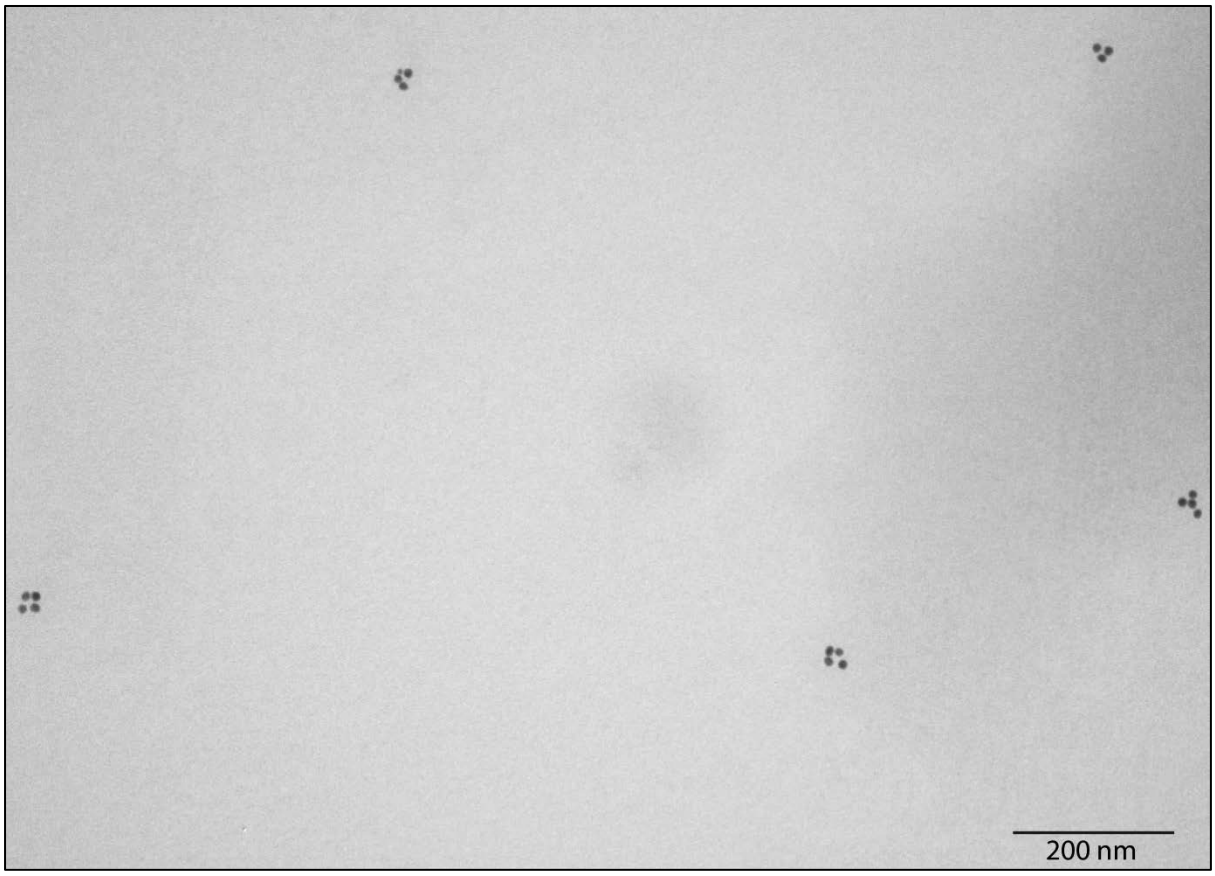

Figure S17: Additional TEM image of crosslinked gold nanoparticle tetrahedral over a larger area of the grid.

S8. Dynamic light scattering and additional UV-Vis spectra

Dynamic light scattering was performed for gold nanoparticle monomers, dimers, trimers and tetrahedra. While there is a significant change in the hydrodynamic radius, no aggregation is observed (**Figure S18**).

It has been discussed previously that small nanoparticles only exhibit limited plasmon coupling between each other at distances dictated by our DNA design. This only leads to a small broadening in the UV-Vis spectrum rather than a significant red-shift of the plasmon resonance.[6] A comparison between dimers, trimers and tetramers in our work, points to similar conclusions (**Figure S19**). The distances between nanoparticles was calculated to 8.8 nm. While for the dimers and trimers the broadening is not very clear, it can be observed for the tetramers.

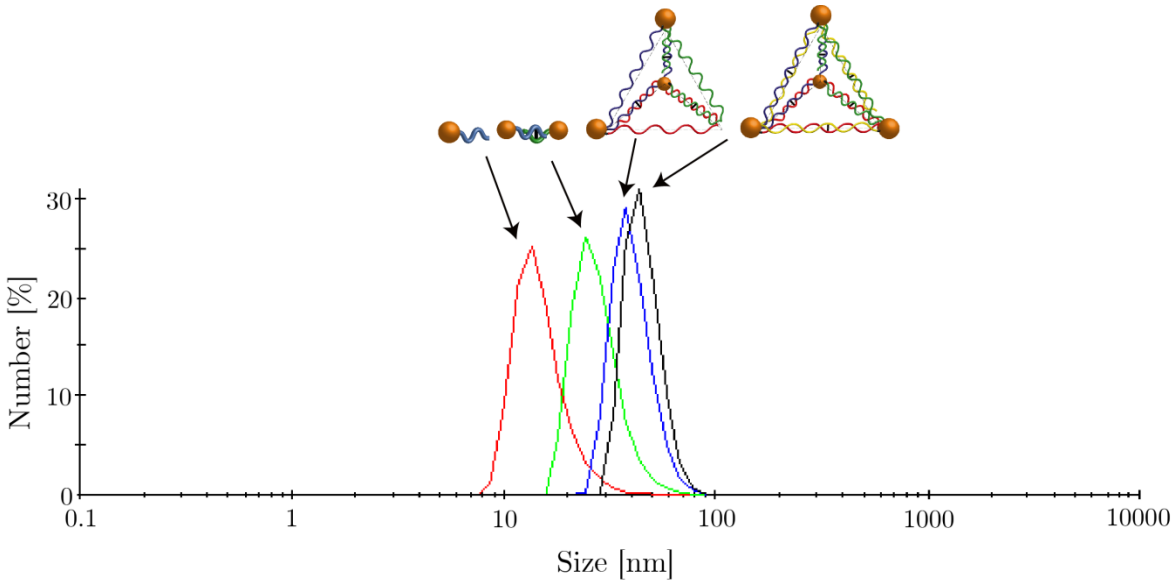

Figure S18: Dynamic light scattering spectra of gold nanoparticle monomers (red), dimers (green), trimers (blue), tetrahedra (black).

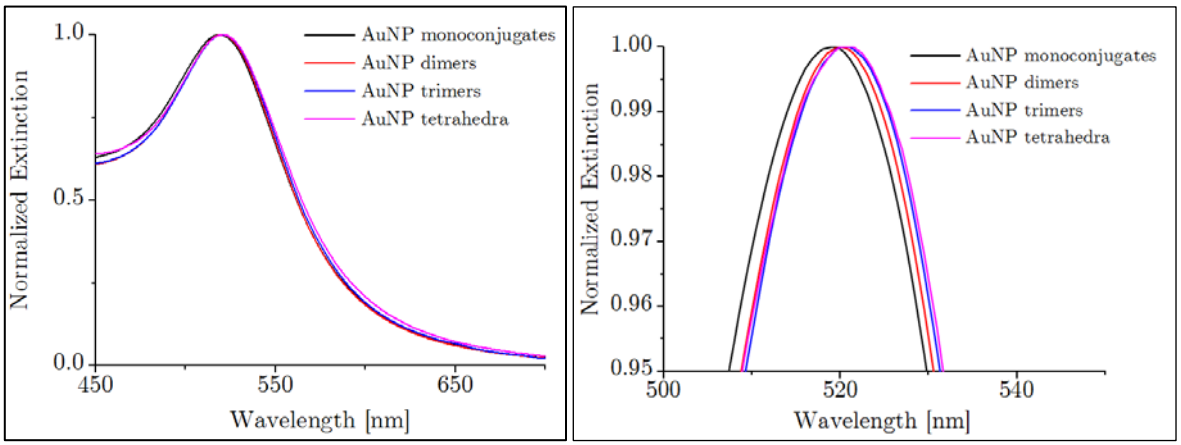

Figure S19: UV-Visible spectrum of gold nanoparticle mono-conjugates, dimers, trimers and tetrahedral structures (left). A magnification of the maximum peaks (right).

References:

(1) Turkevich, J.; Stevenson, P. C.; Hillier, J. *J. Phys. Chem.* **1953**, *57*, 670-673.
(2) Haiss, W.; Thanh, N. T. K.; Aveyard, J.; Fernig, D. G. *Anal. Chem.* **2007**, *79*, 4215-4221.
(3) Loutfy, R. O.; De Mayo, P. *J. Am. Chem. Soc.* **1977**, *99*, 3559-3565.
(4) Schuster, D. I.; Lem, G.; Kaprinidis, N. A. *Chem. Rev.* **1993**, *93*, 3-22.
(5) Burns, J. A.; Butler, J. C.; Moran, J.; Whitesides, G. M. *J. Org. Chem.* **1991**, *56*, 2648-2650.
(6) Lan, X.; Chen, Z.; Liu, B.-J.; Ren, B.; Henzie, J.; Wang, Q. *Small* **2013**, *9*, 2308-2315.